

Separation and location of microseism sources

Aishwarya Moni,¹ David Craig,¹ and Christopher J Bean¹

Received 19 March 2013; revised 10 May 2013; accepted 15 May 2013; published 20 June 2013.

[1] Microseisms are ground vibrations caused largely by ocean gravity waves. Multiple spatially separate noise sources may be coincidentally active. A method for source separation and individual wavefield retrieval of microseisms using a single pair of seismic stations is introduced, and a method of back azimuth estimation assuming Rayleigh-wave arrivals of microseisms is described. These methods are combined to separate and locate sources of microseisms in a synthetic model and then applied to field microseismic recordings from Ireland in the Northeast Atlantic. It is shown that source separation is an important step prior to location for both accurate microseism locations and microseisms wavefield studies. **Citation:** Moni, A., D. Craig, and C. J. Bean (2013), Separation and location of microseism sources, *Geophys. Res. Lett.*, 40, 3118–3122, doi:10.1002/grl.50566.

1. Introduction

[2] Ocean gravity waves are driven by wind and atmospheric pressure systems and generate pressure changes at the seabed [Bromirski, 2009]. These pressure fluctuations generate continuous background seismic noise, called “microseisms,” which are associated with ocean wave activity and are generally stronger in coastal areas, although they are recorded on terrestrial seismic stations throughout the world. Background seismic noise levels increase during periods of increased ocean wave activity. There are two main types of microseisms:

[3] • **Primary**—These have periods of 8–20 s. They are thought to be generated in shallow water by the dynamic interaction between water waves and shoaling seafloor. They can be produced by nonlinear interactions of the ocean wave pressure signal on a sloping seafloor [Hasselmann, 1963].

[4] • **Secondary**—These have periods of 3–10 s. They occur at half the primary wave period and are likely caused by the interference of opposing waves producing a standing wave [Longuet-Higgins, 1950].

[5] Secondary microseisms dominate over primary microseisms, and their amplitudes are proportional to the square of the standing wave height. This makes them sensitive to larger waves/swell. This paper deals with the separation and location of secondary microseisms.

[6] There have been studies aimed at locating primary and secondary microseisms using a variety of methods.

Triangulation using the time delays of arrival of Z component seismograms between station pairs has been used to locate microseism sources [Cessaro, 1994]. f - k analysis has been used with Z components recorded at arrays of stations to determine the slowness and back azimuth [Cessaro, 1994; Cessaro and Chan, 1989; Friedrich et al., 1998; Schulte-Pelkum et al., 2004; Chevrot et al., 2007]. A polarization method, assuming Rayleigh-wave propagation, to calculate the back azimuth by measuring phase differences between horizontal and vertical components has also been used [Schulte-Pelkum et al., 2004; Chevrot et al., 2007; Stutzmann et al., 2009].

[7] Source separation prior to application of location methods has not been studied. Here we demonstrate that this is a crucial step in the process of locating microseisms as they comprise multiple coincidentally active sources. It is also important for determining the spatial and temporal heterogeneity of the microseism wavefield. Source separation will help improve transfer functions developed between land-based recordings of microseisms and wave parameters recorded at ocean buoys. The source separation algorithm used is described in section 2.1, and the location algorithm is briefly discussed in section 2.2. The algorithms are tested on synthetics (section 3) and applied to real data from Ireland, in the Northeast Atlantic (section 4).

2. Algorithms

2.1. Source Separation Using DUET

[8] The algorithm that is used to separate sources in this article is the Degenerate Unmixing Estimation Technique (DUET) [Yilmaz and Rickard, 2004]. This method was designed for acoustic waves to solve the “cocktail party problem,” i.e., separating individual speakers in a room with multiple speakers. This method has been used in a geophysical setting, to separate multiple sources of tremor and long-period events in a volcano [Moni et al., 2012].

2.1.1. Assumptions

[9] *Anechoic Mixing.* Consider a mixture of N source signals, $s_j(t)$, $j = 1, \dots, N$, is received at a pair of stations where only the direct path is present. In this case, without loss of generality, the attenuation and delay parameters of the first mixture, $x_1(t)$, can be absorbed into the definition of the sources. As such, the two anechoic mixtures can be expressed as

$$x_1(t) = \sum_{j=1}^N s_j(t), \quad (1)$$

$$x_2(t) = \sum_{j=1}^N a_j s_j(t - \delta_j), \quad (2)$$

where N is the number of sources, δ_j is the arrival delay between the stations, and a_j is a relative attenuation factor

Additional supporting information may be found in the online version of this article.

¹Seismology Laboratory, School of Geological Sciences, University College Dublin, Dublin, Ireland.

Corresponding author: A. Moni, Seismology Laboratory, School of Geological Sciences, University College Dublin, Dublin, Ireland. (aishwarya.moni@ucd.ie)

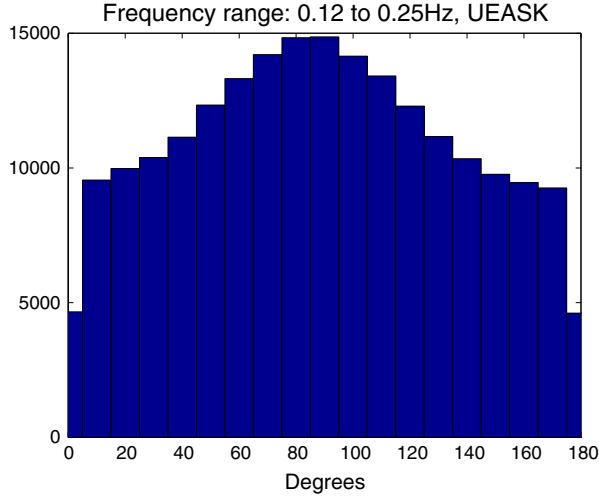


Figure 1. Phase difference between horizontal and vertical components of the microseisms recorded at a seismic station in Western Ireland during the month of October 2011.

corresponding to the ratio of the attenuations of the paths between sources and stations. The anechoic mixing model is not completely realistic, in that it does not represent echoes (that is, multiple paths from each source to each mixture). In spite of this limitation, DUET, which is based on this model, has proven to be quite robust even when applied to echoic mixtures [Rickard, 2007; Moni et al., 2012].

[10] *W-Disjoint Orthogonality.* Two functions $s_j(t)$ and $s_k(t)$ are *W-disjoint orthogonal* if, for a given windowing function $W(t)$, the supports of the windowed Fourier transforms of $s_j(t)$ and $s_k(t)$ are disjoint. That is, at each point in the windowed Fourier transform, at most one source (function $s_j(t)$ or $s_k(t)$) is dominant. The windowed Fourier transform of $s_j(t)$ is defined as

$$\hat{s}_j(\tau, \omega) := \frac{1}{\sqrt{2\pi}} \int_{-\infty}^{\infty} W(t - \tau) s_j(t) e^{-i\omega t} dt. \quad (3)$$

So the *W-disjoint orthogonality* assumption can be stated as

$$\hat{s}_j(\tau, \omega) \hat{s}_k(\tau, \omega) = 0, \forall \tau, \omega, \forall j \neq k. \quad (4)$$

This assumption is the mathematical idealization of the condition that it is likely that every time-frequency point in the mixture with significant energy is dominated by the contribution of one source. *W-disjoint orthogonality* is crucial to

DUET, because it allows for the separation of a mixture into its component sources using a binary mask. Consider the mask which is the indicator function for the support of \hat{s}_j :

$$M_j(\tau, \omega) := \begin{cases} 1 & \text{if } \hat{s}_j(\tau, \omega) \neq 0 \\ 0 & \text{otherwise.} \end{cases} \quad (5)$$

M_j separates \hat{s}_j from the mixture via

$$\hat{s}_j(\tau, \omega) = M_j(\tau, \omega) \hat{x}_1(\tau, \omega), \forall \tau, \omega, \quad (6)$$

where $\hat{x}_1(\tau, \omega)$ is the time-frequency representation of x_1 .

[11] As such, if binary masks for each source could be determined, the sources can be separated by partitioning. In this algorithm, each time-frequency point is labeled with delay differences that explain the time-frequency phase between the two mixtures. These delays cluster into groups, one group for each source.

2.1.2. The Method

[12] The assumptions of anechoic mixing allows the mixing equations (1) and (2) to be rewritten in the time-frequency domain as

$$\begin{bmatrix} \hat{x}_1(\tau, \omega) \\ \hat{x}_2(\tau, \omega) \end{bmatrix} = \begin{bmatrix} 1 & \dots & 1 \\ a_1 e^{-i\omega \delta_1} & \dots & a_N e^{-i\omega \delta_N} \end{bmatrix} \begin{bmatrix} \hat{s}_1(\tau, \omega) \\ \vdots \\ \hat{s}_N(\tau, \omega) \end{bmatrix}. \quad (7)$$

If the further assumption of *W-disjoint orthogonality* is included, at most one source is active at every (τ, ω) , the mixing process can be described for each (τ, ω) as

$$\begin{bmatrix} \hat{x}_1(\tau, \omega) \\ \hat{x}_2(\tau, \omega) \end{bmatrix} = \begin{bmatrix} 1 \\ a_j e^{-i\omega \delta_j} \end{bmatrix} \hat{s}_j(\tau, \omega) \quad (8)$$

for a given j . In the above equation, j depends on (τ, ω) , in that j is the index of the source active at (τ, ω) . The main observation that DUET utilizes is that the ratio of the time-frequency representations of the mixtures does not depend on the source components but only on the mixing parameters associated with the active source component.

$$\forall (\tau, \omega) \in \Omega_j, \frac{\hat{x}_2(\tau, \omega)}{\hat{x}_1(\tau, \omega)} = a_j e^{-i\omega \delta_j}. \quad (9)$$

Here $\Omega := (\tau, \omega) : \hat{s}_j(\tau, \omega) \neq 0$. In this paper, only the relative delay estimates are used, and the relative attenuation estimates are ignored. This is done because the amplitudes recorded by stations are sensitive to local site

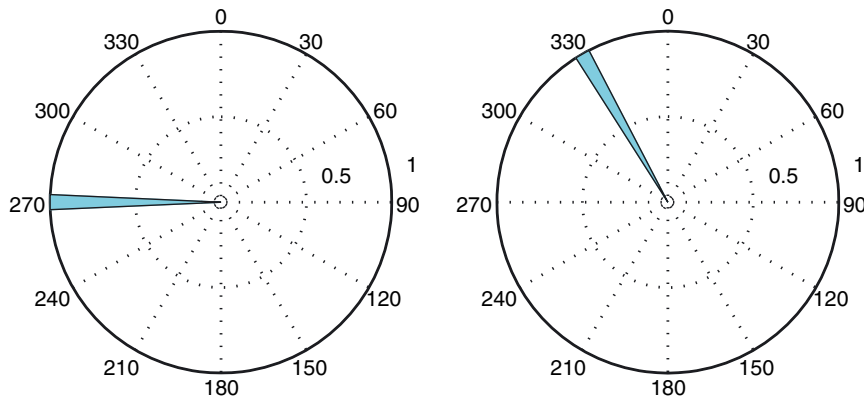


Figure 2. Back azimuth estimation for source 1 (left) and source 2 (right).

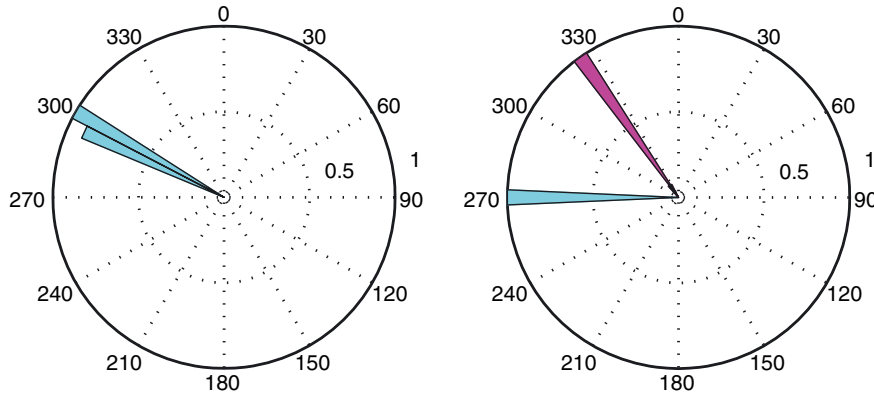


Figure 3. Back azimuth estimation for multiple sources: a combination of source 1 and source 2 (left) and for separated sources (right).

effects; thus, the relative attenuation estimates are not as reliable and accurate as the relative time delay estimates. The mixing parameters (the relative delay estimate in this case) associated with each time-frequency point can be calculated as follows:

$$\delta(\tau, \omega) = -\frac{1}{\omega} \angle \frac{\hat{x}_2(\tau, \omega)}{\hat{x}_1(\tau, \omega)}. \quad (10)$$

The steps taken to separate the sources using DUET are as follows:

[13] 1. Construct the discrete short-time Fourier transform (i.e., spectrogram) [Mallat, 1998] as defined in equation (3) of the signal at each station. In this paper, we use a Hamming window.

[14] 2. Take the ratio of the mixtures to extract the local delay estimate. A delay estimate will result for each time-frequency point.

[15] 3. Generate the histogram of these delays, with each delay bin weighted with the energy of the corresponding time-frequency point.

[16] 4. Find the peak delay for each source.

[17] 5. For each peak found, i.e., for each source, a binary time-frequency mask is then created, based on how close the delay at each time-frequency point is to the peak delays found.

[18] 6. This mask can then be applied to each of the mixtures recorded at each station to get the time-frequency

representation of the separated source recorded at each station.

[19] 7. The separated source signals are then transformed, using the inverse short-time Fourier transform, back to the time domain.

[20] To preserve the phase information during the separation, the algorithm is first run on the Z component seismograms to separate the sources. The binary time-frequency mask calculated for the separation of the Z component seismograms is then applied to the horizontal components to separate the sources. The result is a three-component seismogram at both stations in the pair for each source.

2.2. Source Location

[21] Once separated, we are left with three-component seismograms at both our stations for each separated source. The back azimuth for each separated source is then determined. Microseisms are known to travel primarily with a retrograde elliptical Rayleigh-wave-type particle motion [Haubrich *et al.*, 1963]. To confirm this, the phase difference between the horizontal and vertical calculated using method described in Tanimoto *et al.* [2006] shown in Figure 1.

[22] It can be seen in Figure 1 that there is a peak at 90° phase difference between the horizontal and vertical components. Rayleigh waves have approximately 90° phase difference between horizontal and vertical components.



Figure 4. Back azimuth estimations for sources in the northwest Ireland array before source separation was applied.

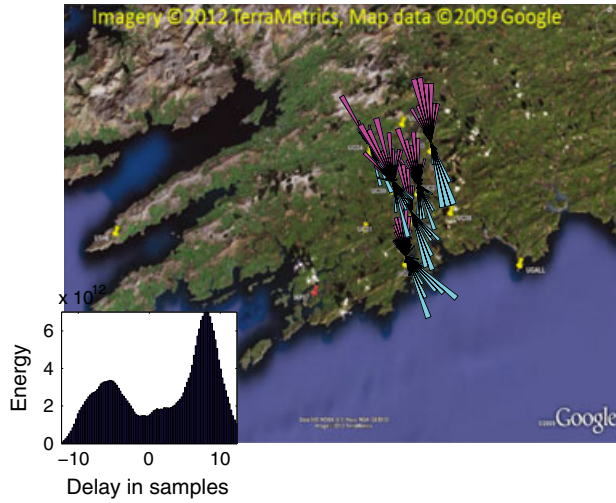


Figure 5. Back azimuth estimations for sources in the southwest Ireland array after source separation using DUET. Four pairs of stations are used for source separation.

The back azimuths (directions of arrival) of the microseisms are calculated by using the 90° phase difference property of Rayleigh waves, by finding the back azimuth which satisfies this phase difference property. The method used in this paper to calculate the back azimuth of the Rayleigh waves is described in *Roberts and Christoffersson* [1990].

3. Synthetic Tests

3.1. Data

[23] Synthetic tests were carried out using a reflectivity method [*Kennett and Kerry*, 1979] combined with the integration method in discrete wave numbers proposed by *Dietrich and Bouchon* [1985] and *Dietrich* [1988]. The data are produced by propagating simultaneously two different ocean noise samples through a laterally homogeneous, stratified, elastic medium. For the model, five layers are used with a free surface above and half space below. P wave velocity goes from 2.5 km/s near the surface to 6.5 km/s in the half space (>25 km depth). S wave velocity varies similarly from 1.45 km/s to 3.8 km/s. There are two seismic stations, located 7 km apart. Source 1 is located at a back azimuth

of 270° and is approximately 60 km from the receivers, and source 2 is located at a back azimuth of 330° and is approximately 70 km from the receivers.

3.2. Results

[24] Figure 2 shows the back azimuths estimated for two individual sources at an individual station using the method of *Roberts and Christoffersson* [1990]. These are estimated accurately as 270° for source 1 and 330° for source 2. Figure 3 (left) shows the back azimuth estimation for a mixture of the two sources. It can be seen that when there are multiple sources present, the back azimuth can then be incorrectly estimated; i.e., it does not point to either contributing source. When one source is dominant (e.g., the energy of one source is more than 5 times the energy of the other sources), the location algorithm points to the dominant source. When the two sources have similar energies, the location algorithm points to neither source.

[25] DUET was used to separate the two sources using the two receivers (approximately one third of a Rayleigh wavelength apart). Figures of the different steps in the separation method for this synthetic example are shown in the supporting information including the separated seismograms. The back azimuth estimation method was then performed on these separated sources. The results are shown in Figure 3 (right). It can be seen that the sources have been separated (magenta indicating source 1 and cyan indicating source 2), and the back azimuths calculated from the separated sources are consistent with the known back azimuths of source 1 and source 2 (shown in Figure 2).

4. Test on Field Data

4.1. Data

[26] The data used in this paper to separate and locate microseisms were recorded on pairs of stations chosen from an 11-element array in southwest Ireland (shown in Figure 4) on 31 January 2012, between 6 A.M. and 8 A.M. The seismograms were filtered between 4 and 8 s periods (0.125–0.25 Hz), i.e., around the secondary microseism.

4.2. Results

[27] The back azimuth estimates for the southwest Ireland array stations, without source separation, are shown in

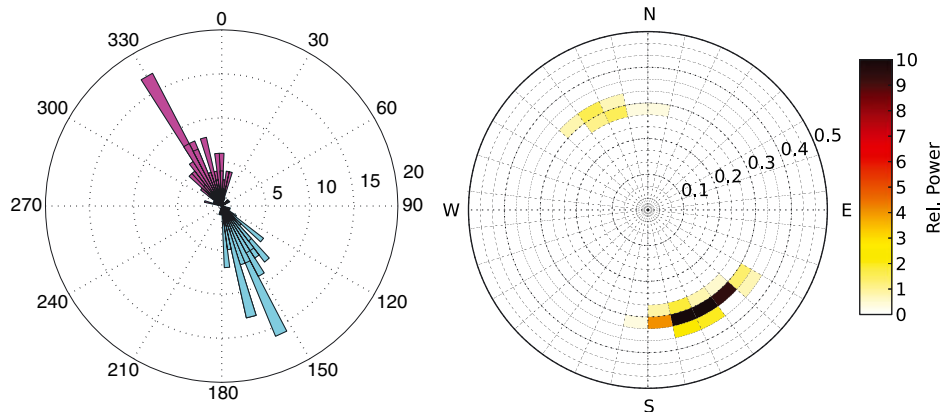


Figure 6. Back azimuth estimation using separated sources from a pair of stations (left) and using f-k analysis on the 11-element southwest Ireland array (right).

Figure 4. The sources seem to be originating from the south-east at most stations, while some stations have a very wide range of back azimuths.

[28] DUET was used to separate sources for four pairs of stations in the array. There were two peaks seen for each of these pairs in the DUET histogram (bottom-left corner in Figure 5), and two sources were separated using these peaks (the source contributing to the peak on the right is stronger). The back azimuths were estimated on these separated sources using horizontal-vertical phase difference analysis. The results of the location of the separated sources are shown in Figure 5. It can be seen that a source seems to originate from the northwest (weaker source) and another from the southeast (stronger source). This is consistent with the back azimuths obtained using f-k analysis on all 11 elements of the array (Figure 6). However, using DUET, we can recover the wavefield associated with each source separately. Similar figures for different time periods are included in the supporting information to show the robustness of the separation method.

5. Conclusions and Future Work

[29] An algorithm for source separation was introduced, and a back azimuth estimation method was briefly described. These methods were tested on synthetic data to test the robustness of the algorithms, and it was shown that separation of sources is essential for the accurate location of microseisms when using the single stations phase difference method. This method was then tested on field data recorded to separate and locate sources. For the majority of existing location methods, periods of time with one dominant source are chosen, and the signals are also filtered to very narrow frequency bands (about 0.2 Hz). This has led to an understanding of the nature of microseisms and their geographical and seasonal patterns. The method outlined in this paper results in separate seismograms for each source at each station. Separating the wavefield will allow for a better understanding of relationships between microseisms and wave climate and noise source heterogeneity for seismic noise correlation imagery studies.

[30] **Acknowledgments.** This material is based upon work supported by the Science Foundation Ireland under Principal Investigator Grant No. 10/IN.1/I3014. The authors would also like to thank their colleagues in the Geophysics Group in University College Dublin for assisting with the fieldwork. The authors would also like to thank R. Roberts for an early version of the back azimuth estimation code and M. Dietrich for the code used for seismic wave simulations. f-k processing is done with the ObsPy toolbox [Beyreuther et al., 2010; Megies et al., 2011]. The authors would also like to thank R. Aster and an anonymous reviewer for their comments which improved the manuscript.

[31] The Editor thanks two anonymous reviewers for their assistance in evaluating this paper.

References

- Beyreuther, M., R. Barsch, L. Krischer, T. Megies, Y. Behr, and J. Wassermann (2010), ObsPy: A python toolbox for seismology, *SRL*, 81(3), 530–533.
- Bromirski, P. (2009), Earth vibrations, *Science*, 324(5930), 1026–1027, doi:10.1126/science.1171839.
- Cessaro, R. K. (1994), Sources of primary and secondary microseisms, *Bull. Seismol. Soc. Am.*, 84(1), 142–148.
- Cessaro, R. K., and W. W. Chan (1989), Wide-angle triangulation array study of simultaneous primary microseism sources, *J. Geophys. Res.*, 94, 15,555–15,563.
- Chevrot, S., M. Sylvander, S. Behanmend, C. Ponsolles, J. M. Lefevre, and D. Paradis (2007), Source locations of the secondary microseisms in Western Europe, *J. Geophys. Res.*, 112, B11301, doi:10.1029/2007JB005059.
- Dietrich, M., and M. Bouchon (1985), Synthetic vertical seismic profiles in elastic media, *Geophysics*, 50(2), 224–234, doi:10.1190/1.1441912.
- Dietrich, M. (1988), Modeling of marine seismic profiles in the t-x and tau-p domains, *Geophysics*, 53(4), 453–465, doi:10.1190/1.1442477.
- Friedrich, A., F. Kruger, and K. Klinge (1998), Ocean generated microseismic noise located with the Grafenberg array, *J. Seismolog.*, 2(1), 47–64.
- Hasselmann, K. A. (1963), Statistical analysis of the generation of microseisms, *Rev. Geophys.*, 1(2), 177–210, doi:10.1029/RG001i002p00177.
- Haubrich, R. A., W. H. Munk, and F. E. Snodgrass (1963), Comparative spectra of microseisms and swell, *Bull. Seismol. Soc. Am.*, 53, 27–37.
- Kennett, B. L. N., and N. J. Kerry (1979), Seismic waves in a stratified half-space, *Geophys. J. Roy. Astr. Soc.*, 57, 557–583.
- Longuet-Higgins, M. S. (1950), A theory of the origin of microseisms, *Phil. Trans. Roy. Soc. London*, A(243), 1–35.
- Mallat, S. G. (1998), *A Wavelet Tour of Signal Processing*, pp. 92–98, Academic, San Diego, CA.
- Megies, T., M. Beyreuther, R. Barsch, L. Krischer, and J. Wassermann (2011), Obspy: What can it do for data centers and observatories? *Ann. Geophys.*, 54(1), 47–58.
- Moni, A., C. J. Bean, I. Lokmer, and S. Rickard (2012), Source separation on seismic data, *IEEE Signal Process. Mag.*, 29(3), 16–28.
- Rickard, S. (2007), *The DUET Blind Source Separation Algorithm*, pp. 217–241, Makino, S., T.-W. Lee, and H. Sawada (eds), Blind Source Separation, Springer-Verlag, Berlin.
- Roberts, R. G., and A. Christoffersson (1990), Decomposition of complex single-station three-component seismograms, *Geophys. J. Int.*, 103, 55–74.
- Schulte-Pelkum, V., P. S. Earle, and F. L. Vernon (2004), Strong directivity of ocean-generated seismic noise, *Geochem. Geophys. Geosyst.*, 5, Q03004, doi:10.1029/2003GC000520.
- Stutzmann, E., M. Schimmel, G. Patau, and A. Maggi (2009), Global climate imprint on seismic noise, *Geochem. Geophys. Geosyst.*, 10, Q11004, doi:10.1029/2009GC002619.
- Tanimoto, T., S. Ishimaru, and C. Alvizuri (2006), Seasonality in particle motion of microseisms, *Geophys. J. Int.*, 166, 253–266.
- Yilmaz, O., and S. Rickard (2004), Blind separation of speech mixtures via time-frequency masking, *IEEE Trans. Signal Process.*, 52(7), 1830–1847.